Vibrational Spectroscopy

International Edition: DOI: 10.1002/anie.201600603
German Edition: DOI: 10.1002/ange.201600603

A Symmetric Recognition Motif between Vicinal Diols: The Fourfold Grip in Ethylene Glycol Dimer

*Franz Kollipost, Katharina E. Otto, and Martin A. Suhm**

Abstract: *Ethylene glycol has a transiently chiral, asymmetric global minimum structure, but it favors a highly symmetric, achiral dimer arrangement which has not been considered or found in previous quantum-chemical studies. Complementary FTIR and Raman spectroscopy in supersonic jets allows for the detection and straightforward assignment of this four-fold hydrogen-bonded dimer, which introduces an interesting supramolecular binding motif for vicinal diols and provides a strong case for transient chirality synchronization.*

Carbohydrates are among the most versatile molecules employed by nature in molecular recognition processes and their biomimetic detection is challenging.[1] When reducing their molecular complexity to a minimum, one naturally arrives at vicinal diols. Among them, the simplest representative ethylene glycol has even been detected in interstellar space.[2] Ethylene glycol or 1,2-ethanediol is a particularly valuable model system for the study of multiple hydrogen-bonded dimers and carbohydrate interactions,[3] because it allows for a vast range of quantum-chemical options to be explored. Indeed, the question of its preferred dimer structure has been addressed repeatedly by theory,[4–6] but not by experimental techniques. Because of the torsional flexibility of ethylene glycol, there are several possibilities how the four OH groups of the dimer can engage in hydrogen bonds. None of the previously proposed structures involves more than three hydrogen bonds among these OH groups.[4–11]

We present unambiguous combined IR and Raman spectroscopic evidence that ethylene glycol in fact forms an S_4-symmetric and thus non-polar and achiral dimer with four equivalent hydrogen bonds. Using Gaussian 09,[12] an extensive search of the intermolecular potential-energy hypersurface at B3LYP-D3(BJ)/6-311+G(2d,p) level (in short B3LYP) confirms that this structure wins over all triply hydrogen-bonded dimer structures by a substantial energy margin.

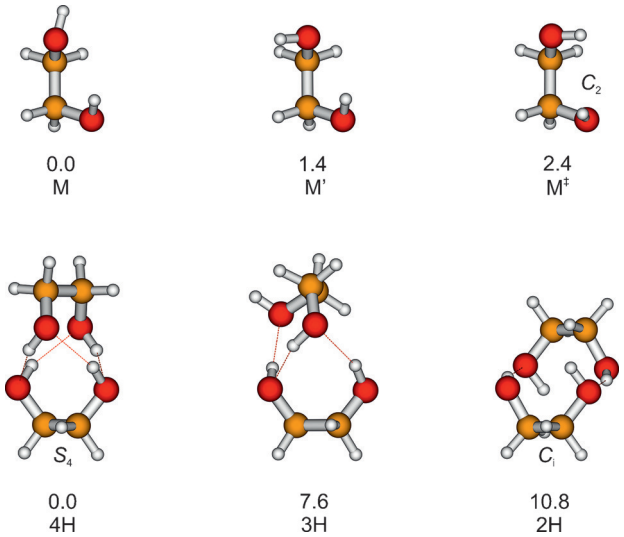

Figure 1. Calculated representative structures of ethylene glycol on the B3LYP-D3(BJ)/6-311+G(2d,p) level of computation with harmonically corrected relative energies in kJ mol^{-1}. The two most stable monomer geometries are denoted M and M′ and differ only in the orientation of the free OH group. Also shown is the lowest C_2-symmetric transition-state structure M‡ (without zero-point energy in the barrier mode). The most stable dimer is 4H with four intermolecular hydrogen bonds (see the Supporting Information for a rotating representation). 3H is the most stable dimer of a variety of energetically close structures with three intermolecular hydrogen bonds (see Figure S5). The eighth located minimum structure in the energy sequence of the dimer features two intermolecular hydrogen bonds and is named 2H.

The two lowest monomer structures found at the harmonically zero-point energy-corrected B3LYP level are depicted in Figure 1. They have in common a *gauche* OCCO backbone, a weakly hydrogen-bonded OH group, and a free OH group pointing in *trans* (M) or *gauche* (M′) direction relative to the C–C backbone. These monomer conformations are chiral and differ only by 1.4 kJ mol^{-1} at B3LYP level, making both of them potentially observable in a seeded adiabatic jet expansion. They have been investigated previously in much detail,[13–25] mostly by microwave spectroscopy,[13–20] and experimental estimates for their energy difference are rather close to our theoretical prediction, with 1.4(4) and 2.5(5) kJ mol^{-1}.[16,20] In jet experiments, typically only M is observed in substantial abundance because of efficient conformational relaxation,[18] whereas at room temperature, M′ is also populated. Donor–acceptor OH torsional tunneling splits the levels by 0.2 and 0.05 cm^{-1}, respectively.[17,18] IR spectroscopy has confirmed the non-equivalent OH groups[21,26] and irradiation of matrix-isolated ethylene glycol has given access to higher-lying conforma-

[*] Dr. F. Kollipost, Dr. K. E. Otto, Prof. Dr. M. A. Suhm
Institut für Physikalische Chemie
Georg-August-Universität Göttingen
Tammannstr. 6, 37077 Göttingen (Germany)
E-mail: msuhm@gwdg.de

Supporting information, including experimental and computational details of the reaction paths and dimer structures, and the ORCID identification number(s) for the author(s) of this article are available under http://dx.doi.org/10.1002/anie.201600603.

tions.[22–25] In the liquid phase, a *trans* backbone[27–29] as well as intermolecular and thus less frustrated hydrogen bonds become more important.[4] In the solid, all hydrogen bonds are intermolecular.[30]

The key to unambiguous symmetric dimer detection is a combination of linear Fourier transform infrared (FTIR) spectroscopy and linear Raman scattering based on intense 532 nm excitation,[31–33] both coupled to slit jet expansions of ethylene glycol in an excess of helium carrier gas to adiabatically cool and dimerize the diol without environmental distortion. The linearity and non-selectivity of the complementary techniques ensures that the relative abundance of different species can be judged reliably. Only atomic species are invisible to this spectroscopic combination.

The FTIR spectrum for an expansion of 100 ppm ethylene glycol in 0.7 bar He at room temperature (see Figure S1 in the Supporting Information) reveals two monomer signals at 3689 and 3636 cm^{-1} that correlate nicely with conformation M, when compared to a gas-phase overtone[21] extrapolation (see Table S2). A single signal attributable to dimers (D) is observed near 3513 cm^{-1} at a low signal-to-noise ratio despite probing a 600 mm long expansion zone (see Figure S1).[33] The dimer signal was optimized by employing a 10 mm double slit nozzle at elevated temperature,[32] which allows for a higher monomer concentration. The spectrum, in which the dimer signal now exceeds the monomer signal, is displayed in Figure 2. It also shows a weak second dimer peak at a 39 cm^{-1} lower wavenumber, together with further, even weaker signals which may stem from minor conformations, larger clusters, or small impurities. No significant absorption due to M′ is observed. The situation changes when switching to Raman scattering (Figure 2, lowest trace, inverted), which allows to probe the expansion much closer to the nozzle exit, where metastable monomer conformations may still survive. Indeed, a second pair of monomer transitions due to M′ (not yet detected unambiguously in interstellar space[34]) is now observed at 3657 and 3624 cm^{-1}, shifted to lower wavenumbers relative to the respective M bands. The strongest IR dimer peak is completely absent in the Raman spectrum, pointing at a high symmetry of the underlying structure. The weaker IR peak is present in the Raman spectrum as well, ruling out inversion symmetry. The strongest Raman peak is further down-shifted in wavenumber by 30 cm^{-1} and has no IR counterpart, again pointing at a high symmetry situation in this dimer. The experimental spectra are thus consistent with a single dominant dimer structure of high symmetry without inversion center.

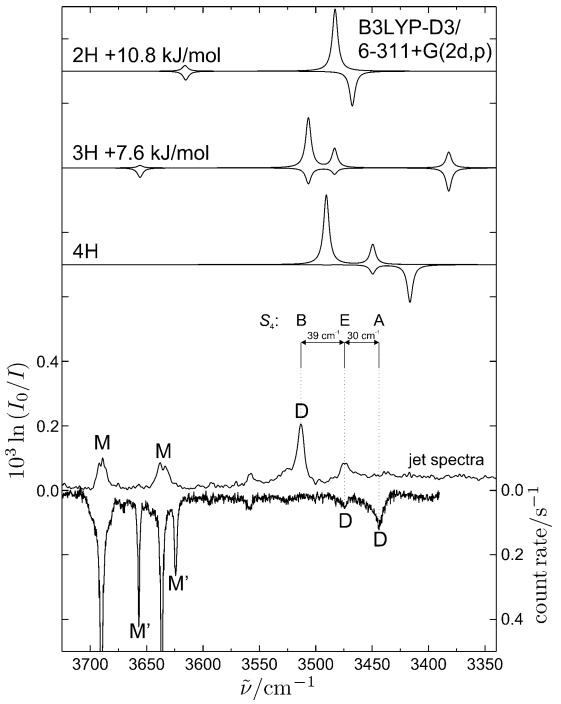

Figure 2. Lower panel: Two experimental jet spectra of ethylene glycol from heated nozzle expansions. The upright trace is the FTIR spectrum and the inverted trace shows the Raman spectrum. Upper panel: Scaled harmonic wavenumber (×0.9569, to match the average monomer positions) predictions for the dimer structures 4H, 3H, and 2H. Their intensities are scaled assuming a dimer concentration of 10% compared to the experimental monomer concentration and are facing upwards for IR signals and downwards for Raman bands.

A systematic search of the dimer conformational energy landscape reveals at least 13 structures in a 12 kJ mol^{-1} interval (see Figure S5). By far the most stable structure with a zero-point-corrected dissociation energy of 51.4 kJ mol^{-1} is denoted 4H (Figure 1; see the Supporting Information for a rotating representation), because it exhibits four hydrogen bonds, all equivalent, all intermolecular, and all significantly strained. The underlying monomer fragments have C_2 symmetry and are thus distorted from the two most stable monomer structures M and M′. Their electronic relaxation energy to the global monomer minimum amounts to 6.5 kJ mol^{-1}, showing that the dipolar arrangement of the OH groups is not very favorable. The monomer units must have opposite chirality in order to form the 4H structure—this includes opposite signs for the OCCO dihedrals in the two monomer units. If two monomers with the same sense of rotation in their OCCO dihedrals meet, which happens in every second collision, they can at best form a less stable, non-symmetric, triply hydrogen-bonded structure (which is not observed in the experiment). Alternatively, one of the monomers has to invert over a substantial OCCO torsional racemization barrier. Thus, the almost exclusive observation of a symmetric dimer in the spectra points at a pronounced case of chirality synchronization in the recognition process, opposite in sign to the case of trifluoroethanol.[35]

7.6 kJ mol^{-1} higher or 15% less stable than the 4H structure, a triply hydrogen-bonded structure, similar to structures discussed before,[4–6,9] is located and denoted 3H (Figure 1). Again, all its hydrogen bonds are intermolecular, but one OH is dangling. Remarkably, this second most stable structure is also heterochiral with respect to the OCCO torsion angle. The first homochiral pairing of OCCO angles occurs for the third most stable structure at a dissociation energy of 42.8 kJ mol^{-1} (3Hb, see Figure S5), 17% less stable than 4H. This underscores a pronounced racemization pressure on ethylene glycol units upon pair formation. Ten more structures are found in an energy interval of 9.2 to 11.9 kJ mol^{-1} above the global minimum structure—four of them with opposite and six with the same sign of the OCCO

torsion angle. They feature between two and four intermolecular hydrogen bonds (see Figure S5). The most stable dimer structure with only two intermolecular hydrogen bonds (2H, Figure 1) is the eighth in the energetic sequence at 10.9 kJ mol^{-1} above 4H. Additionally, 2H features two monomer-like weak intramolecular contacts and has C_i symmetry. It is thus easily ruled out as being responsible for the observed dominant dimer signals for energy and symmetry reasons. 3H can also be ruled out by comparing its simulated spectra (top traces of Figure 2, IR upright and Raman inverted) with experiment, after scaling the harmonic fundamental predictions to the correct average monomer position (× 0.9569). While the dangling OH absorption might be hidden underneath the monomer signals in these non-size-selected spectra, the predicted simultaneous IR and Raman activities for all three bonded transitions is in sharp contrast to the observed selectivity for IR or Raman in two of the observed bands. The other dimer structures found in the 8.6 to 11.9 kJ mol^{-1} energy interval can also be ruled out due to their predicted band positions and intensities (see Table S3). Furthermore, it would require sizeable barriers for conformational interconversion to trap dimer isomers with these high-energy penalties, given that the monomers relax so efficiently at least with respect to OH torsion. It is therefore beyond doubt that the spectra reveal the global minimum structure 4H for the ethylene glycol dimer, for which the predicted intensity and coupling pattern agrees perfectly with experiment.

The four equivalent OH bonds in the 4H dimer couple into three different motion patterns following the irreducible representations of the S_4 group, ranging from concerted stretching to alternating stretch and compression. The S_4 symmetry dictates an IR-inactive totally symmetric (A) vibration in which all four OH groups stretch in phase and induce large Raman activity by polarizability modulation. The two other modes of B and degenerate E symmetry are IR- and also weakly Raman-active. In tetramers of alcohols with a more or less planar OH-group arrangement, the E band dominates the IR spectrum.[31] In the dimer of ethylene glycol, the situation is reversed, because the OH groups are tilted out of the plane by steric constraints. Due to the alternating monomer origin of the OH groups in the hydrogen-bonded ring, the two E modes are naturally localized in one of the monomers.

The energy of each of the four hydrogen bonds in the ethylene glycol dimer may be estimated by adding to the calculated electronic dissociation energy of the dimer (63.9 kJ mol^{-1}) twice the preparation energy for the monomer in the dimer geometry (2 × 6.5 kJ mol^{-1}). Each hydrogen bond contact is thus worth almost 20 kJ mol^{-1} despite being significantly distorted. This is comparable to the interaction energy in unconstrained $(HF)_2$ and only 20 % less than in the methanol dimer,[36] showing that cooperativity compensates for steric constraints.

More insight into the bonding situation can be obtained by analyzing the experimental splitting pattern of the A, B, and E levels revealed by the combination of IR and Raman OH-stretching spectroscopy. In a simple Hückel-type analysis,[31] the coupling constant between two neighbouring OH groups W_1 is 17 cm^{-1}. This is significantly less than the 29 cm^{-1} found for the unconstrained methanol tetramer[31] or the 26 cm^{-1} found in the water tetramer,[37] as expected due to the distortion of the hydrogen bonds in the ethylene glycol dimer. More interesting is the coupling W_2 between opposite OH groups, which are not directly bound to each other. In the methanol (water) tetramer, W_2 is still 11 cm^{-1} (8 cm^{-1}) although the limiting dipole–dipole interaction between the two OH groups is slightly repulsive. This is explained by the pronounced cooperativity in the ring which favors a simultaneous stretching of the two opposing OH groups even though the dipole–dipole interaction through space may be unfavorable. In the dimer of ethylene glycol, W_2 is −2 cm^{-1} (confirmed by the quantum-chemical calculations, see Table S3). Such a negative coupling among second-nearest neighbors is unusual for hydrogen-bonded rings. Qualitatively, it means that if one OH group is stretched, the opposite one (on the same molecule in the ethylene glycol case) prefers to shrink, although they are connected in a cooperative network. Obviously, the cooperativity along the corrugated hydrogen-bonded ring in ethylene glycol dimer is not sufficient to compensate for this through-space effect. This is also a consequence of the rather short distance between the two OH units, caused by steric constraints of the OCCO backbone. The average position of the OH fundamentals in ethylene glycol dimer is about 200 cm^{-1} higher in wavenumber than for the methanol tetramer, another consequence of the steric strain. The dimer bands are significantly more narrow than predicted by a simple correlation of red shift with homogeneous line width.[38] In summary, two ethylene glycol units are held together by a cooperatively enhanced cyclic hydrogen bond pattern, but the spectra contain ample information on the significant hydrogen bond strain present in this construction due to the chemical link between the carbon atoms, which is of course absent in the methanol tetramer.

The molecular recognition motif detected here between two vicinal diols is not expected to survive further aggregation. Indeed, the solid and liquid states of ethylene glycol are known or believed to form extended intermolecular networks.[4,29,30,39,40] Furthermore, we are not aware of any report of this motif in crystal packings of carbohydrates, which usually prefer less strained infinite cooperative chains.[41,42] However, it is conceivable that an artificial receptor based on such a vicinal diol recognizes corresponding vicinal OH groups in carbohydrates through such a fourfold binding motif, at least in a solvent-depleted environment. More importantly, this motif deserves to be investigated further by advanced and approximate quantum-chemical methods because it can serve as a test case for the correct molecular modeling of bent cooperative hydrogen bonding.

The surprising aspect in the almost exclusive formation of the 4H dimer structure from two monomer units is not so much the rearrangement of four OH torsional angles, which is facilitated by quantum tunneling. It is the forced inversion of the OCCO torsional angle upon aggregation in close to 50 % of all encounters, a process which is known to be strongly hindered in monomeric jet expansions of the related 1,2-dimethylglycol.[43] For ethylene glycol, the required barrier is

close to 20 kJ mol^{-1}[44] (see also Figure S4), too high to be overcome by carrier gas collisions. In the dimer, it is conceivable that this barrier is lowered. Indeed, we find that the transition state from the lowest CC-homochiral dimer (3Hb) to the CC-heterochiral global minimum structure only requires 14.0 kJ mol^{-1} of activation and passes through a CC-homochiral dimer with four hydrogen bonds (Figure S6). This barrier reduction alone is not sufficent to explain the dominance of CC-heterochiral dimers in the supersonic expansion, but the initial dimerization energy of at least 20 kJ mol^{-1} per monomer may easily transform one of the OCCO angles into its enantiomer. The underlying process, for which our experimental spectra provides clear evidence, is thus a case of autocatalytic racemization. Our finding encourages molecular dynamics modeling of the racemization dynamics in sticking CC-homochiral collisions of ethylene glycol. The quality requirements for the underlying force fields are not too high, because the effect is so robust. The energy gap from the S_4 structure to the next-higher conformations of the ethylene glycol dimer is so large that it is unlikely that any reasonable level of theory interchanges the sequence. Indeed, even without dispersion corrections, the B3LYP calculation for the six lowest dimers preserves the same energetic order, although the 4H structure loses about one half of its energy advantage. This is in contrast to the compact S_4 symmetric arrangement of racemic methyl lactate tetramer,[45] which B3LYP without dispersion correction fails to predict as a global minimum structure.

One might also consider an alternative mechanism, which is occasionally discussed[46,47] and profits from a relatively high diol concentration in the supersonic jet expansions. Collision of a metastable and thus reactive CC-homochiral dimer with an enantiomeric monomer could result in the more stable CC-heterochiral dimer and a surplus monomer carrying away the excess energy (and chirality) via a transient trimer. Because some of these and other transient trimers are expected to be stabilized by further rare gas collisions, the absence of significant trimer signals in the presented vibrational spectra makes this mechanism somewhat less likely.

It will be interesting to extend this combined IR and Raman study to vicinal propane and butane diols to see how the added methyl groups influence the molecular recognition by their steric repulsion and dispersion interactions. The step to 1,2-propanediol[48] also introduces interesting non-transient chirality recognition effects.

Acknowledgements

This work has been supported by the Deutsche Forschungsgemeinschaft (DFG, grant number SU 121/2). We greatly acknowledge help from Anja Poblotzki.

Keywords: dimers · hydrogen bonds · molecular recognition · racemization · vibrational spectroscopy

How to cite: *Angew. Chem. Int. Ed.* **2016**, *55*, 4591–4595
Angew. Chem. **2016**, *128*, 4667–4671

[1] A. P. Davis, R. S. Wareham, *Angew. Chem. Int. Ed.* **1999**, *38*, 2978–2996; *Angew. Chem.* **1999**, *111*, 3160–3179.
[2] J. M. Hollis, F. J. Lovas, P. R. Jewell, L. H. Coudert, *Astrophys. J.* **2002**, *571*, L59.
[3] O. Guvench, A. D. MacKerell, Jr., *J. Phys. Chem. A* **2006**, *110*, 9934–9939.
[4] I. Bakó, T. Grósz, G. Pálinkás, M. C. Bellissent-Funel, *J. Chem. Phys.* **2003**, *118*, 3215–3221.
[5] N. Breslavskaya, M. Rodnikova, I. Solonina, S. Dolin, T. Val′kovskaya, *Russ. J. Inorg. Chem.* **2012**, *57*, 1563–1569.
[6] R. M. Kumar, P. Baskar, K. Balamurugan, S. Das, V. Subramanian, *J. Phys. Chem. A* **2012**, *116*, 4239–4247.
[7] Y. Elkadi, L. Adamowicz, *Chem. Phys. Lett.* **1996**, *261*, 507–514.
[8] S. Pal, T. K. Kundu, *ISRN Phys. Chem.* **2013**, 753139.
[9] A. Y. Samuilov, A. R. Valeev, F. B. Balabanova, Y. D. Samuilov, A. I. Konovalov, *Russ. J. Inorg. Chem.* **2013**, *49*, 1723–1727.
[10] M. Krest′yaninov, A. Titova, A. Zaichikov, *Russ. J. Phys. Chem. A* **2014**, *88*, 2114–2120.
[11] F. H. Tukhvatullin, U. N. Tashkenbaev, A. Jumabaev, H. A. Hushvaktov, A. A. Absanov, B. Hudoyberdiev, *Ukr. J. Phys.* **2014**, *59*, 219.
[12] M. J. Frisch et. al., Gaussian 09, Revision D.01, Gaussian Inc., Wallingford CT, 2013.
[13] K.-M. Marstokk, H. Møllendal, *J. Mol. Struct.* **1974**, *22*, 301–303.
[14] E. Walder, A. Bauder, H. H. Günthard, *Chem. Phys.* **1980**, *51*, 223–239.
[15] W. Caminati, G. Corbelli, *J. Mol. Spectrosc.* **1981**, *90*, 572–578.
[16] P.-E. Kristiansen, K. Marstokk, H. Møllendal, *Acta Chem. Scand. Ser. A* **1987**, *41*, 403–414.
[17] D. Christen, L. Coudert, R. Suenram, F. Lovas, *J. Mol. Spectrosc.* **1995**, *172*, 57–77.
[18] D. Christen, L. Coudert, J. Larsson, D. Cremer, *J. Mol. Spectrosc.* **2001**, *205*, 185–196.
[19] D. Christen, H. S. P. Müller, *Phys. Chem. Chem. Phys.* **2003**, *5*, 3600–3605.
[20] H. S. P. Müller, D. Christen, *J. Mol. Spectrosc.* **2004**, *228*, 298–307.
[21] D. L. Howard, P. Jørgensen, H. G. Kjaergaard, *J. Am. Chem. Soc.* **2005**, *127*, 17096–17103.
[22] T.-K. Ha, H. Frei, R. Meyer, H. H. Günthard, *Theor. Chim. Acta* **1974**, *34*, 277–292.
[23] H. Frei, T.-K. Ha, R. Meyer, H. H. Günthard, *Chem. Phys.* **1977**, *25*, 271–298.
[24] H. Takeuchi, M. Tasumi, *Chem. Phys.* **1983**, *77*, 21–34.
[25] C. G. Park, M. Tasumi, *J. Phys. Chem.* **1991**, *95*, 2757–2762.
[26] P. Buckley, P. A. Giguère, *Can. J. Chem.* **1967**, *45*, 397–407.
[27] K. Krishnan, R. S. Krishnan, *Proc. Indian Acad. Sci. Sect. A* **1966**, *64*, 111–122.
[28] H. Matsuura, M. Hiraishi, T. Miyazawa, *Spectrochim. Acta Part A* **1972**, *28*, 2299–2304.
[29] C. Murli, N. Lu, Z. Dong, Y. Song, *J. Phys. Chem. B* **2012**, *116*, 12574–12580.
[30] D. Chopra, T. N. Guru Row, E. Arunan, R. A. Klein, *J. Mol. Struct.* **2010**, *964*, 126–133.
[31] R. Wugt Larsen, P. Zielke, M. A. Suhm, *J. Chem. Phys.* **2007**, *126*, 194307.
[32] M. Albrecht, J. Will, M. A. Suhm, *Angew. Chem. Int. Ed.* **2010**, *49*, 6203–6206; *Angew. Chem.* **2010**, *122*, 6339–6342.
[33] M. A. Suhm, F. Kollipost, *Phys. Chem. Chem. Phys.* **2013**, *15*, 10702–10721.
[34] N. Brouillet, D. Despois, X.-H. Lu, A. Baudry, J. Cernicharo, D. Bockelée-Morvan, J. Crovisier, N. Biver, *Astron. Astrophys.* **2015**, *576*, A129.
[35] J. Thomas, Y. Xu, *J. Phys. Chem. Lett.* **2014**, *5*, 1850–1855.
[36] M. Heger, M. A. Suhm, R. A. Mata, *J. Chem. Phys.* **2014**, *141*, 101105.

[37] K. E. Otto, Z. Xue, P. Zielke, M. A. Suhm, *Phys. Chem. Chem. Phys.* **2014**, *16*, 9849 – 9858.
[38] K. Takahashi, *Phys. Chem. Chem. Phys.* **2010**, *12*, 13950 – 13961.
[39] D. Belashchenko, M. Rodnikova, N. Balabaev, I. Solonina, *Russ. J. Phys. Chem. A* **2014**, *88*, 94 – 102.
[40] A. Kaiser, O. Ismailova, A. Koskela, S. E. Huber, M. Ritter, B. Cosenza, W. Benger, R. Nazmutdinov, M. Probst, *J. Mol. Liq.* **2014**, *189*, 20 – 29.
[41] G. A. Jeffrey, J. Mitra, *Acta Crystallogr. Sect. B* **1983**, *39*, 469 – 480.
[42] C. P. Brock, *Acta Crystallogr. Sect. B* **2002**, *58*, 1025 – 1031.
[43] S. Bocklitz, M. A. Suhm, *Z. Phys. Chem. (Muenchen Ger.)* **2015**, *229*, 1625 – 1648.
[44] T.-S. Yeh, Y.-P. Chang, T.-M. Su, I. Chao, *J. Phys. Chem.* **1994**, *98*, 8921 – 8929.
[45] T. B. Adler, N. Borho, M. Reiher, M. A. Suhm, *Angew. Chem. Int. Ed.* **2006**, *45*, 3440 – 3445; *Angew. Chem.* **2006**, *118*, 3518 – 3523.
[46] J. Zischang, J. J. Lee, M. A. Suhm, *J. Chem. Phys.* **2011**, *135*, 061102.
[47] A. Mahjoub, K. Le Barbu-Debus, A. Zehnacker, *J. Phys. Chem. A* **2013**, *117*, 2952 – 2960.
[48] R. Friedemann, A. Fengler, S. Naumann, U. Gromann, *J. Mol. Struct. THEOCHEM* **1995**, *357*, 217 – 223.

Received: January 19, 2016
Published online: March 1, 2016

